Journal of Bodywork and Movement Therapies (2007) **11**, 159–167

ELSEVIER

Journal of **Bodywork and Movement Therapies**

www.intl.elsevierhealth.com/journals/jbmt

BIOMECHANICAL THEORETICAL ANALYSIS

Viscoelastic behavior of human fasciae under extension in manual therapy

Hans Chaudhry, Ph.D.[a,f], Chien-Yueh Huang, Ph.D.[b,*], Robert Schleip, M.A.[c], Zhiming Ji, Ph.D.[d], Bruce Bukiet, Ph.D.[e], Thomas Findley, M.D., Ph.D.[a,f]

[a]*Department of Biomedical Engineering, New Jersey Institute of Technology, Newark, NJ 07102, USA*
[b]*Otto H. York Department of Chemical Engineering, New Jersey Institute of Technology, Newark, NJ 07102, USA*
[c]*Department of Applied Physiology, Ulm University, Albert-Einstein-Allee 11, 89069 Ulm, Germany*
[d]*Department of Mechanical Engineering, New Jersey Institute of Technology, Newark, NJ 07102, USA*
[e]*Department of Mathematical Sciences, Center for Applied Mathematics and Statistics, New Jersey Institute of Technology, Newark, NJ 07102, USA*
[f]*War-Related Illness and Injury Study Center, VA Medical Center, East Orange, NJ 07018, USA*

Received 22 April 2006; received in revised form 14 August 2006; accepted 30 August 2006

KEYWORDS
Manual therapy;
Viscoelasticity;
Human fasciae;
Plastic deformation

Summary The basic field equations for viscoelastic soft tissues are employed for exploring the relationship between time varying mechanical stresses and dynamic deformations of human fasciae in manual therapy. The predicted stress range for plastic deformation of plantar fascia, based on the viscoelastic model is close to experimental data. Fascia lata (in vitro) and plantar fascia (in vitro) are found to exhibit similar behavior, irrespective of how the fasciae are deformed.

Manual therapists should avoid increasing deformation with time. It is desirable to produce deformation which should become constant after some time, and be applied for the duration up to 60 s. The therapists may apply almost the same load to produce the same plastic deformation for plantar fascia and fascia lata. Greater loads are needed to produce the same strain with higher rate of deformation. The data presented in this paper may also be useful for surgeons in planning the orientation of fascia in knee and hip replacement surgeries.

ABSTRACT

The basic field equations for viscoelastic soft tissues are employed for exploring the relationship between time varying mechanical stresses and dynamic deformations of human fasciae in manual therapy. The predicted stress range for plastic deformation of plantar fascia, based on the viscoelastic model is close to experimental data. Fascia lata (in vitro) and plantar fascia (in vitro) are found to exhibit similar behavior, irrespective of how the fasciae are deformed.

Manual therapists should avoid increasing deformation with time. It is desirable to produce deformation which should become constant after some time, and be applied for the duration up to 60 seconds. The therapists may apply almost the same load to produce the same plastic deformation for plantar fascia and fascia lata. Greater loads are needed to produce the same strain with higher rate of deformation. The data presented in this paper may also be useful for surgeons in planning the orientation of fascia in knee and hip replacement surgeries.

Keywords: Manual Therapy, Viscoelasticity, Human Fasciae, Plastic Deformation.

Key Points

- This study explores the tissue deformation forces in human fascia during manual therapy. It also puts these forces into a relationship with their effect on viscoelastic tissue deformation.
- Fascia lata and plantar fascia require similar forces for the same amount of deformation.
- Perhaps not surprisingly: less dense fasciae, like the superficial nasal fascia, require lesser forces for plastic deformation than denser fasciae like the fascia lata.
- In order to achieve a viscoelastic deformation during manual intervention, without causing tissue damage, it is suggested that there should be no slow increase in the applied force. Rather it is recommended that a fairly constant force be maintained, for up to 60 s, in order to allow for a plastic stress relaxation response of the tissue.

1. INTRODUCTION

Fascia is the dense fibrous connective tissue which joins muscles, bones and organs and is a continuous network throughout the body. It plays an important role in transmitting mechanical forces in human posture. Several forms of manual fascial therapies have been developed which aim to improve postural alignment and other expressions of musculoskeletal dynamics (Rolf 1989), (Varela & Frenk 1987); (Cantu & Gordin 1992) and (Ward 1993). The mechanical properties of ex-vivo rat superficial fascia (subcutaneous tissue) under uni-axial tension have recently been investigated due to its potential importance in a variety of therapies involving mechanical stretch (Iatridis et al 2003). The mechanical properties of in-vitro human superficial nasal fascia and nasal periosteum were investigated by (Zeng et al 2003) to determine under which layer silicon implants should be inserted for better results of aesthetic plastic surgery to correct congenital saddle-nose and flat nose. Similarly the mechanical properties of in-vitro and in-vivo properties of plantar fascia and fascia lata have also been investigated by(Wright & Rennels 1964) and (Magnusson et al 2001). These studies are based upon the hypothesis that the fasciae are elastic. However, the fasciae exhibit viscoelastic behavior (Yahia et al 1993).

The viscoelastic properties of the human lumbodorsal fascia have been studied by (Yahia et al 1993) to provide better understanding of the mechanical response of the lumbodorsal fascia to dynamic and static traction loadings. (Iatridis et al 2003) studied the viscoelastic mechanical properties of ex-vivo rat subcutaneous tissue in uniaxial tension with incremental stress relaxation experiments and concluded that the response was linear and viscoelastic under uniaxial tension. (Zhang 2005) developed a new method for evaluating the viscoelastic properties of biological connective tissues such as tendons and ligaments.

The purpose of the present paper is to evaluate the dynamic stresses (and therefore the applied loads) resulting from the dynamic deformations in manual therapy by using the data provided by (Iatridis et al 2003), (Zeng et al 2003); (Wright & Rennels 1964) and (Magnusson et al 2001) for superficial nasal and dense fascia lata and plantar fascia. The theoretical analysis of the dynamic stresses originated from such a scientific basis will be very helpful to manual therapists who presently use their intuition to apply the stresses (loads) to produce a desired deformation in the fasciae. The analysis was performed based on the constitutive equations developed by (Fung 1984) with the strain energy functions valid for the viscoelastic bodies of soft tissues such as the fasciae employed above.

2. METHODS

2.1. Basic field equations for viscoelastic biological tissue

2.1.1. Extension

We assume the deformation produced by the manual therapy technique of extension along the x^1 axis (Fig.1) to be given by

$$y^1 = \lambda x^1, \tag{1}$$

where λ is the stretch ratio; the y^i axes in the deformed state coincide with the x^i axes in the un-deformed state. The longitudinal stress σ_1 thus produced under stretch λ will be determined from the equation for viscoelastic case (see Appendix,. eqn.14):

$$\sigma_1 = \sigma_{11} = C_1 \int_{-\infty}^{t} G(t-\tau) e^{Q_{VE}} [F_1(\lambda) + F_2(\lambda)] \frac{d\lambda}{d\tau} d\tau \tag{2}$$

and for purely elastic case from (Green and Zerna, 1968)

$$\sigma = 2C_1C_2(\lambda^2 - \frac{1}{\lambda}) e^{C_2(I_1-3)}, \quad I_1 = \lambda^2 + \frac{2}{\lambda} \tag{3}$$

where C_1, C_2 are elastic constants.

= 0.915 MPa and C_2 = 83.000 for fascia lata (in vivo).

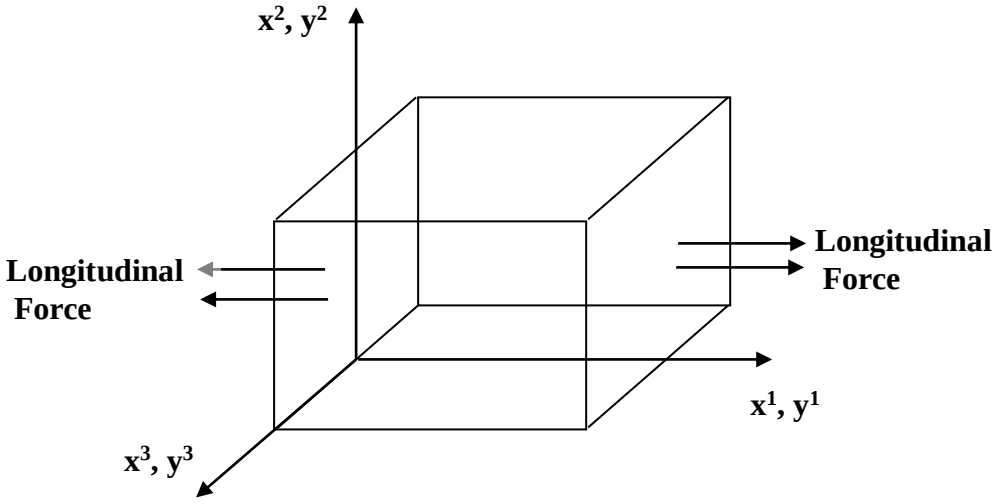

Figure 1. Three dimensional fascial element subjected to longitudinal force in the un-deformed state. The axes (x^1, x^2, x^3) in the un-deformed state coincide with the axes (y^1, y^2 , y^3) in the deformed state.

These are evaluated for various fasciae as given below:
C_1 = 0.0327 MPa and C_2 =8.436 for fascia lata;
C_1 = 0.9313 MPa and C_2 = 61.775 for plantar fascia (in vitro); C_1 = 2.883 MPa and C_2 = 32.419 for fascia lata (in vitro); C_1

3. RESULTS

3.1.

The deformation functions for strain, E employed in our calculations are given below:

$E=\beta t$, $\beta=0.001$, i.e., strain increases linearly with time t, (4)

$E=0.1002[1-e^{-\beta t}]$; $\beta=0.05$, i.e., strain levels off with time t. (5)

We evaluate the dynamic stresses for fascia lata (in vivo and in vitro), plantar fascia and superficial nasal fascia (in vitro) with Eq.(2) and appropriate materials parameters and give the results in Figs 3-6 .

The stress-time curves of various tissues based on the deformation function Eq. (4) are shown in Figure 3. The strain-time curve is presented in the inset. Curves of fascia lata in-vitro and in-vivo are close when t<40 second (i.e. $\lambda < 1.04$), however, the latter is about three times the former at t=100 second. Generally speaking, the curves for both fascia lata in-vitro and plantar fascia in-vitro are roughly similar. The stress of the superficial nasal fascia increases linearly with time (and λ), instead

convex as observed in the other curves. Superficial nasal fascia is much softer compared to other tissues in this study.

Figure 4 shows the stress-time curves of various tissues based on the deformation function Eq. (5). Despite the strain-time curve (inset) levels off at large t, all stress curves exhibit relaxation after a maximum stress is reached. The relaxation decays show the viscous dissipation of the energy stored in the tissues. The curves of fascia lata (in vitro) and (in vivo) are close when t<10 seconds (i.e. $\lambda < 1.04$), however, the latter is about three times of the former at t =100 second. Generally speaking, the curves for both fascia lata (in vitro) and plantar fascia (in vitro) are also roughly similar. We also note that plastic deformation (3%-4,13%, Threlkeld 1992) occurs between 7-11 seconds, and the relaxation after the maximum stress, occurs at about 60 seconds.

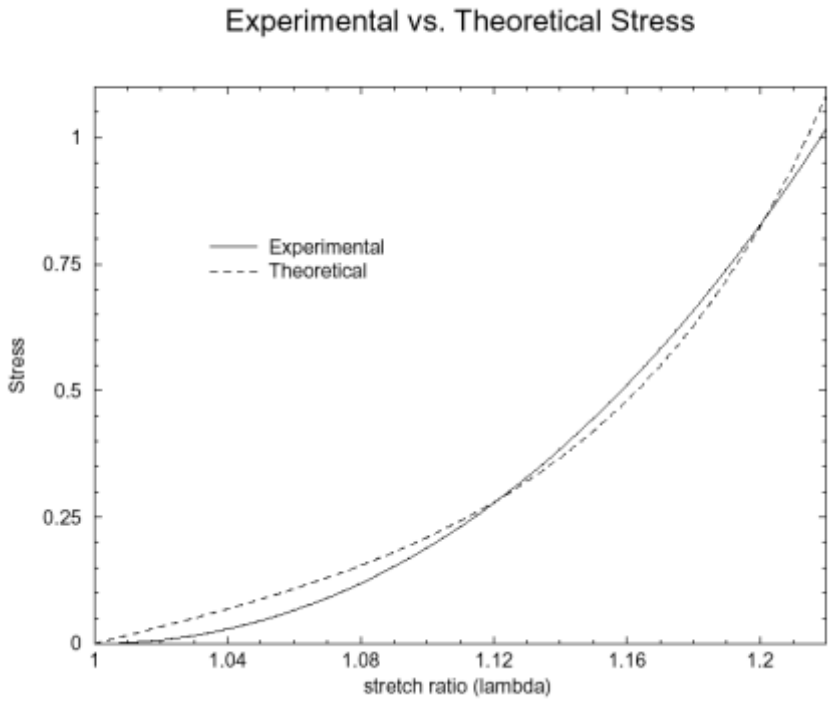

Figure 2. Experimental and theoretical stress-stretch ratio curves for superficial nasal fascia. Unit of stress are in MPa.

Figure 5 shows the prediction of the stress-strain curves of fascia lata (in vitro) under various strain rates. For comparison, the stress calculated from the elastic model (Eq. (3)) is also presented in the grey curve. As expected from the standard model of viscoelasticity employed in this study, the higher the strain rate is, the closer the stress-strain curves to the elastic limit. We note that as the strain levels off along with the time, the relaxation mechanism becomes dominant and the decay of the stress is observed.

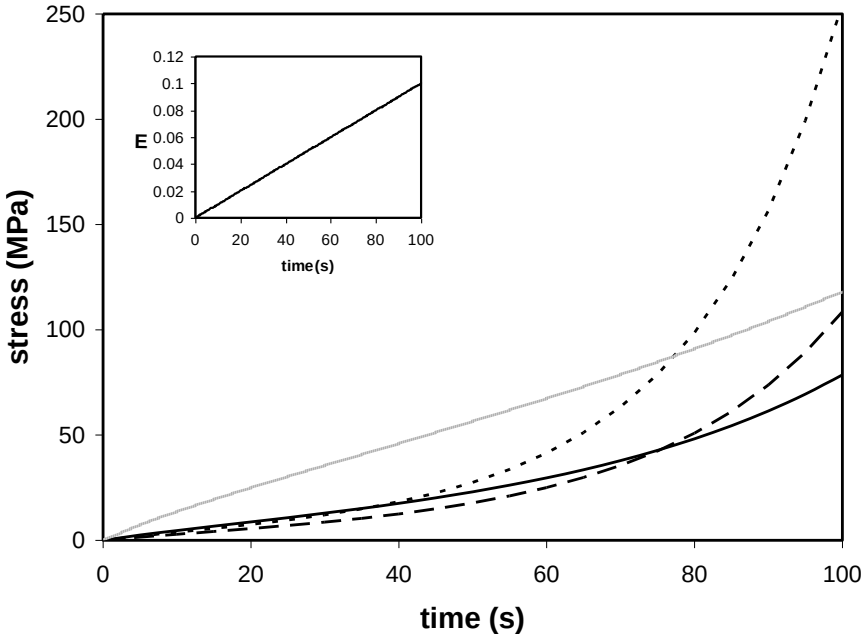

Figure 3. σ_1 (MPa) versus time (s) calculated from the deformation function Eq. (22) for four different cases. Solid curve: fascia lata (in vitro); short dashed curve: fascia lata (in vivo); long dashed curve: plantar fascia (in vitro); grey curve: superficial nasal fascia (magnified by 1000 times). The strain-time curve is presented in the inset.

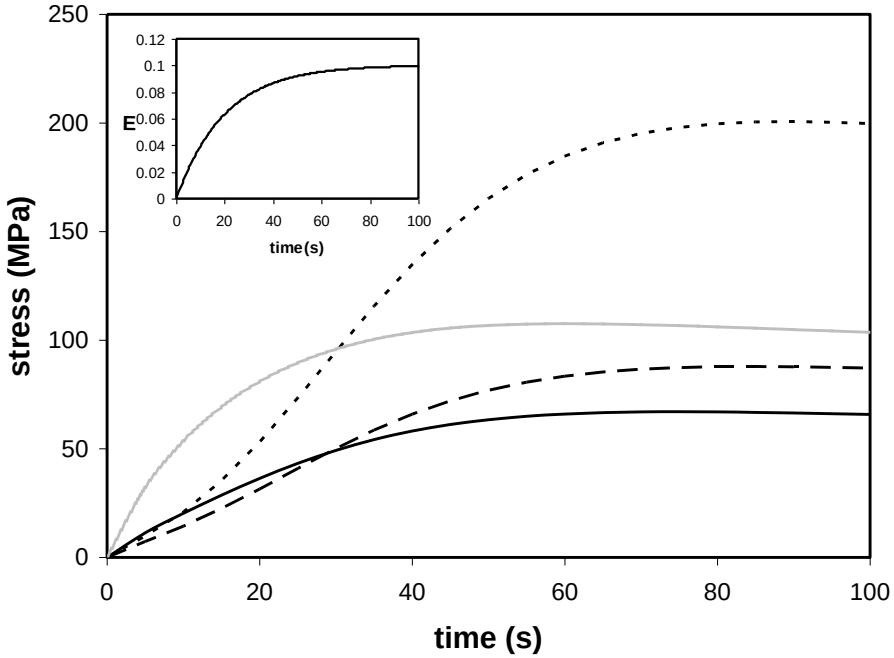

Figure 4. σ_1 (MPa) versus time (s) calculated from the deformation function Eq. (23) for four different cases. Solid curve: fascia lata (in vitro); short dashed curve: fascia lata (in vivo); long dashed curve: plantar fascia (in vitro); grey curve: superficial nasal fascia (magnified by 1000 times). The strain-time curve is presented in the inset.

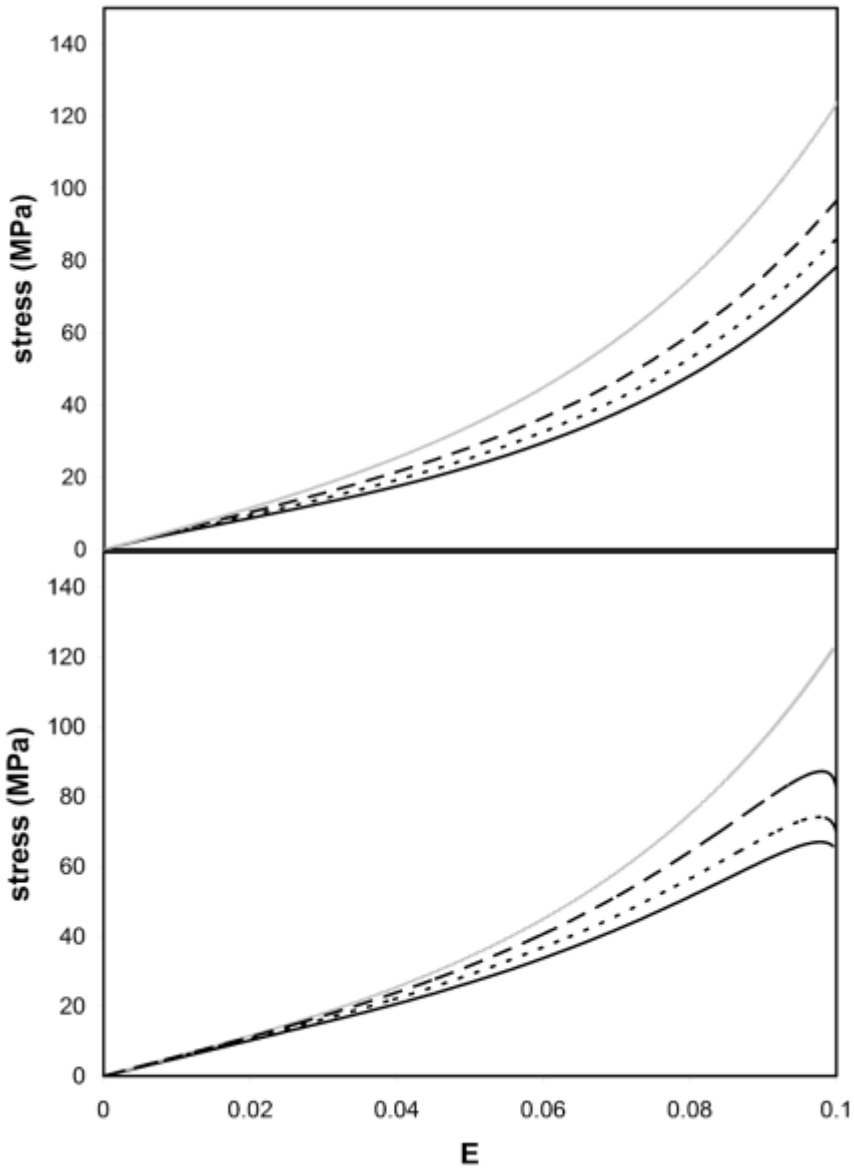

Figure 5. Predicted stress-strain curves of fascia lata (in vitro) under various strain rates. (a) From the bottom, the σ_1-λ curves represent the deformation functions $E=\beta t$ according to solid: $\beta=0.001$; short dashed: $\beta=0.002$; long dashed: $\beta=0.005$; grey: elastic model (Eq.(6)). (b) From the bottom, the σ_1-λ curves represent the deformation functions $E=0.1002\ [1-e^{-\beta t}]$ according to solid: $\beta=0.05$; short dashed: $\beta=0.1$; long dashed: $\beta=0.3$; grey: elastic model (Eq.(6).

Figure 6 shows the sensitivity of the relaxation parameters. It is found that the sensitivity to the span of the relaxation spectrum is small. However, the sensitivity to the coefficient C0 is rather significant. The sensitivity is expected to be larger if a longer relaxation period is allowed or oscillatory deformations are applied. As C0 increases, a larger deviation from the elastic model due to viscoelastic dissipation is observed. However, in the range of plastic deformation, our results show no changes

due to variation of C0 from 0.2 to 0.3. When C0=0 i.e. no viscoelastic dissipation, the stress is solely from the elastic response. The small difference between the C0=0 curve and the elastic model (dotted curve) is due to the perturbative expansion employed in our derivation.

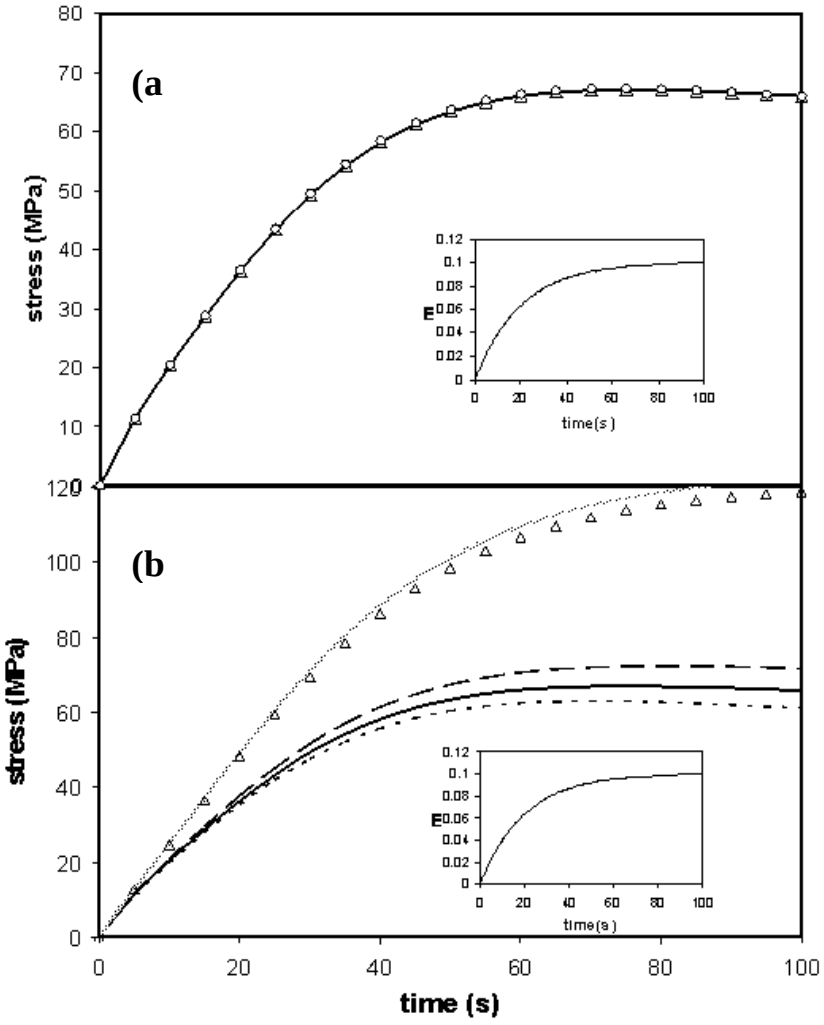

Figure 6. Predicted stress-strain curves of fascia lata (in vitro) calculated from the relaxation function Eq.(21) with various relaxation parameters. The deformation function Eq.(23) is shown in the inset. (a) Solid curve: q_{2C}=98.2; triangle: q_{2C}=110.4;
circle: q_{2C}=12.2. (b) Solid curve: C0 =0.25; short dashed curve: C0=0.3; long dashed curve: Co=0.2; triangle: C0 =0; dashed curve: elastic model (Eq. (6)).

3.1 Comparison of Predicted Stresses and Experimental data

We now use equation (2) to predict the longitudinal stress for plastic deformation (3% - 4.13% strain), the range of deformation where the palpable sensation of a tissue release is reported by manual therapists when working on the dense plantar and fascia lata. These are given in Table 1. This is done to check if the

predicted stress range required to produce elongation plastic deformation (3% - 4.13%) as micro-failure region for dense fascia according to (Threlkeld 1992) agrees with the experimental stresses measured (788N/cm^2 - 1997N/cm^2). Note that 3% elongation occurs at 4 mm displacement when the microfailure begins, and 4.13% is interpolated when microfailure ends at 5.5 mm displacement (Threlkeld1992, Fig.5). We use the stress values (not the force values) due to a wide variation of the cross sectional area of fasciae, since the thickness in the areas of cross section (width multiplied by thickness) often varies with the subject's age (Goh et al 2003). The experimental stress values given above have been evaluated by dividing the force values (246 N- 623 N) by the estimated area of cross section of 0.312 cm^2 (Goh et al 2003). The ranges of predicted stress values for plastic deformation for the three dense fasciae are given in table 1 for comparison with the known experimental stress ranges.

Fascia Type	**Stress Range (N/cm^2) for plastic deformation by the viscoelastic model**
Plantar Fascia (in vitro)	876.50-1348.89 (predicted)
Fascia Lata (in vitro)	1307.05-1864.67 (predicted)
Fascia Lata (in vivo)	1230.69-1999.61 (predicted)
Connective tissue (in vitro) Threlkeld (1992)	788.00 - 1997.00 (experimental)

Table 1 Predicted longitudinal stress for plastic deformation (3% - 4.13% strain), the range reported by manual therapists when working on the dense plantar and fascia lata.

We do not include the predicted results for superficial nasal fascia in this table since it is not dense fascia. The differences of the above predicted values from the experimental values may have arisen because the mechanical properties of the fascias in the current case may be different from those of the vitro sample mentioned by (Threlkeld 1992). Moreover the experimental stress range was obtained by assuming a linear stress-strain relation (Threlkeld 1992), whereas our predictions are based on the actual non-linear stress-strain relation. However, note that the predicted stress

range for plastic deformation of plantar fascia (in vitro), based on the viscoelastic model is close to experimental finding.

3.2. Predicted Stiffness for the Fasciae

Since the predicted stresses for the viscoelastic model are close to the experimental findings, we use the viscoelastic stresses and strains of the viscoelastic model to evaluate the predicted stiffness for all the fasciae for the plastic deformation region (where palpable sensation for tissue release is felt**)** from Figures **(?).** The predicted stiffness for plantar fascia (in- vitro), fascia lata (in- vitro), fascia lata (in-vivo), superficial nasal fascia (in-vitro) are 403.75 MPa, 476.6 MPa, 657.2 MPa, and 1.1 MPa respectively. Note that there is not much difference of stiffness between plantar fascia (in vitro) and fascia lata (in vitro). Therefore, manual therapists may apply almost the same load to produce the same plastic deformation for plantar fascia and fascia lata. The stiffness of fascia lata (in vivo) is about one and half times that of fascia lata (in vitro). The stiffness of superficial nasal fascia is at 1.1MPa, tiny compared to the others.

4. CONCLUSION

The behavior of fascia lata (in vitro) and plantar fascia (in vitro) is very similar, in general, irrespective of how the fasciae are deformed. However, fascia lata (in vivo) is much stiffer (about one and half times that of fascia lata (in vitro)). It is also observed that for soft superficial nasal fascia, the stress versus time relation is linear unlike the non linear behavior of fascia lata and plantar fascia. The mechanical responses of the dense fasciae approaches the elastic behavior with a higher strain rate, meaning that greater stresses (and therefore greater loads) are needed to produce the same strain with a higher rate of deformation.

The predicted stress range for plastic deformation of plantar fascia , based on the viscoelastic model is close to the experimental finding for connective tissue. If the strain increases with time, stress also increases and the tissues can reach a near failure level. Therefore, manual therapists should avoid increasing deformation with time. In contrast if the strain levels off with increasing time, stress relaxation is observed after a maximum stress is reached; this happens at about 60 seconds. Therefore, it is

advisable to produce deformation which should become constant after some time (e.g. Eq. (5)) and be applied for duration up to about 60 seconds. This conclusion is consistent with the fact that no increase in flexibility of the tissues is observed with increasing time (Bandy et al 1997) and agrees with the common practice in manual therapy.

It is difficult to analyze the viscoelastic behavior of fasciae under compression and shear at this point because the shear relaxation functions in a three dimensional space are not known. However, experimental one-dimensional extension relaxation function is known and can be applied. Despite the fact that there are no available mechanical properties for anisotropic and non-homogeneous fasciae, this study presents a first attempt to predict the stresses (and therefore the applied loads) by assuming the fasciae to be isotropic and homogeneous**.** Since we have extracted the one-dimensional relaxation function determined experimentally along the dominant direction of the fiber orientation, the predicted stresses in this study are accurate, and are near the reported stress range in experiments without adjusting the parameters,

REFERENCES

Bandy WD, Irion MB, Briggler M, Oct 1997 The effect of time and frequency of static stretching on flexibility of the hamstring muscles. Physical Therapy 77, 10 ; 1090-7.

Cantu R I, Gordin AJ, 1992. Myofascial manipulation-theory and clinical application. Aspen Publishers, Gaithersburg, Maryland.

Demiray H, 1976 Stresses in Ventricular Wall. J. Appl. Mechanics. 43: 194-197.

Fung FC, 1984 Biodynamics Circulation. Springer- Verlag, NewYork

Fung FC, 1994 A First Course in Continuum Mechanics, Third Edition, Prentice Hall, Englewood Cliffs, New Jersey.

Goh LA, Chhem RK, Wang SC, Chee T, 2003. Iliotibial band thickness: sonographic measurements in asymptomatic volunteers. J. Clin.Ultrasound 31: 239-244.

Green AE, Zerna W 1968. Theoretical Elasticity. Clarendon Press, Oxford.

Hochmann D, Diesing P, Boenick U, 2002. Evaluation of measurement systems for determining therapeutic effectiveness of anti-decubitus ulcer devices. Biomed.Tech. 47: Suppl. 1, Pt. 2, 816-819.

Iatridis J, Wu J, Yandow J, Langevin H, 2003. Subcutaneous tissue mechanical behavior is linear and viscoelastic under uniaxial tension. Connect. Tissue Res. 44: 208-217.

Magnusson SP, Aaggaard P, Rosager S, Poulsen D, Kjaer M. 2001. Load –displacement properties of the human triceps surae aponeurosis in vivo. J. Physiol. 531: Pt. 1, 277-288.

Rolf IP 1989. Rolfing: reestablishing the natural alignment and structural integration of the human body for vitality and well-being. Healing Arts Press, Rochester, Vermont,

Threlkeld AJ 1992. The effects of manual therapy on connective tissues. Phys. Ther. 72: 893-902.

Varela FJ, Frenk S, 1987. The organ of form: towards a theory of biological shape. Journal of Social Biology and Structure 10: 73-83.

Ward RC, 1993. Myofascial release concepts, in: Basmajian, V., Nyberg, R., (Eds.), Rational Manual Therapies. Williams & Wilkins, Baltimore, pp. 223- 241.

Wright DG, Rennels DC 1964. A study of the elastic properties of plantar fascia. J. Bone Joint Surg. Am. 46: 482-492.

Yahia LH, Pigeon P, DesRossiers EA, 1993. Viscoelastic properties of the human lumbodorsal fascia.

J. Biomech. Eng. 15: 425- 429.
Zeng YJ, Sun X, Yang J, Wu W, Xu X, Yan Y. 2003. Mechanical properties of nasal fascia and periosteum. Clin. Biomech. 18: 760 -764.,
Zhang G, 2005. Evaluating the viscoelastic properties of biological tissues in a new way. J. Musculoskelet Neuronal Interact. 5(1): 85-90.

APPENDIX

In order to determine the dynamic stress responding to the applied dynamic extension for viscoelastic fasciae, a quasi-linear constitutive equation (Fung 1984) is employed to address the viscoelastic behavior in biological soft tissues. This can be written as:

$$\sigma_{ij}(\mathrm{x},t) = \int_{-\infty}^{t} G_{ijkl}(t-\tau)\frac{\partial \sigma_{kl}^{(e)}(\mathrm{x},\tau)}{\partial \tau}\,d\tau - p\delta_{ij}\,, \tag{1}$$

where $\sigma^{(e)}$ is the pseudo-elastic stress and a function of strain, which in turn is a function of position **x** and time t; G_{ijkl} is the tensor of relaxation function; τ is a dummy variable for the integration from the beginning (t = -infinity ?) (Fung,1994, p 200) of the deformation to the present time t. *p* is the pressure originated from the incompressibility constraint and the boundary conditions. In the case of uniaxial extension, there is no external stress applied on the perpendicular directions to the extension; *p* must balance the deformation induced stresses along the perpendicular directions. The pseudo-elastic stress can be further expressed as a partial derivative of a pseudo-strain energy function:

$$\sigma_{kl}^{(e)}(\mathrm{x},\tau) = \frac{\partial(\rho_o W)}{\partial E_{kl}(x,t)}\,; \tag{2}$$

E_{kl} is Green's strain function. $\rho_o W$ is a nonlinear pseudo-strain potential energy for a pseudo-elastic body. Here, the off-diagonal components are assumed symmetric, i.e. $E_{ij}=E_{ji}$. Therefore, there are 6 independent components, designated here as $E_1=E_{11}$, $E_2=E_{22}$, $E_3=E_{33}$, $E_4=E_{12}$, $E_5=E_{13}$, and $E_6=E_{23}$. We employ the strain energy function W, for soft tissues (Demiray, 1976) given by

$$W = C_1[e^{Q_{EL}} - 1]; \quad Q_{EL} = C_2(I_1 - 3)\,. \tag{3}$$

Here C_1, C_2 are elastic constants to be determined for superficial fascia, plantar fascia, and fascia lata. This is done by using the least square method to minimize the difference between the theoretical and experimental longitudinal stresses for these fasciae. For the theoretical stress, we use eqn.3 above, and for the experimental stress, we use the data given in (Zeng, 2003) for superficial nasal fascia, and for plantar and fascia lata, we use the data given in (Wright, et al. 1964; Magnusson, et al. 2001) to determine the best values of C_1 and C_2. As an illustration, the case of superficial nasal fascia is given

(Fig.2). The computed values are C_1 = 0.0327 MPa and C_2 =8.436 for fascia lata; C_1 = 0.9313 MPa and C_2 = 61.775 for plantar fascia (in vitro); C_1 = 2.883 MPa and C_2 = 32.419 for fascia lata (in vitro); C_1 = 0.915 MPa and C_2 = 83.000 for fascia lata (in vivo).

Now, to the lowest order of the strains, the exponent Q_{EL} obeys the following quadratic expression:

$$Q_{EL} = \alpha_{mn} E_m E_n\,, \tag{4}$$

where α_{mn} is a constant and E_m is the mth strain. Substituting Eqs.(2)-(4) into Eq.(1), the stress function can be written as:

$$\sigma_i(\mathrm{x},t)=\int_{-\infty}^{t} G_{im}(t-\tau)\mathrm{C}_1\, e^{Q_{VE}}\left(\frac{\partial Q_{VE}}{\partial E_m}\frac{\partial Q_{VE}}{\partial E_n}+\frac{\partial^2 Q_{VE}}{\partial E_m \partial E_n}\right)\frac{\partial E_n(\mathrm{x},\tau)}{\partial \tau}d\tau - p(\delta_{i1}+\delta_{i2}+\delta_{i3})$$

,

(5)

where the abbreviations of the stresses are designated in a similar fashion, i.e. $\sigma_1=\sigma_{11}$, $\sigma_2=\sigma_{22}$, $\sigma_3=\sigma_{33}$, $\sigma_4=\sigma_{12}$, $\sigma_5=\sigma_{13}$, and $\sigma_6=\sigma_{23}$ and δ_{ij} is a Kronecker delta function. Note that the pressure is isotropic and appears only in the normal directions. Eq. (5) is a general constitutive equation for linearly viscoelastic bodies. This equation can be readily applied to experiments where stress-strain relations are measured from where the materials parameters such as the coefficients C_1 and α_{mn} can be retrieved. For a uniaxial extension system, Q_{EL} can be derived from $\mathrm{Q_{EL}}= \mathrm{C}_2\,(\mathrm{I}_1\text{-}3)$ under small stretch ratios. Such a task is achieved by a direct comparison of the coefficients in Taylor's expansions of $\mathrm{Q_{EL}}$ around $\lambda=1$. Assuming uniaxial extension is along the spatial coordinate 1, Eq.(4) can be written as:

$$\begin{aligned} Q_{EL} &= \alpha_{11}E_1^{\,2}+4\alpha_{12}E_1E_2+4\alpha_{23}E_2E_3 \\ &= \alpha_1(\lambda^2-1)^2+\alpha_2(\lambda^2-1)(\frac{1}{\lambda}-1)+\alpha_3(\frac{1}{\lambda}-1)^2\,, \end{aligned} \tag{6}$$

where the Green's strains E_{ij} for isotropic incompressible tissues are given below

$$\begin{aligned} &E_{11}=\frac{1}{2}(\lambda^2-1); \\ &E_{22}=E_{33}=\frac{1}{2}(\frac{1}{\lambda}-1); \\ &E_{ij}=0, \qquad \text{if } i\neq j. \end{aligned} \tag{7}$$

It is assumed that $\alpha_{12}=\alpha_{21}=\alpha_{13}=\alpha_{31}$ and $\alpha_{22}=\alpha_{33}=\alpha_{23}=\alpha_{32}$ in the derivation due to the argument of symmetry. The expansions were carried out to the 4th order and the coefficients in Eq.(12) were given as:

$$\alpha_1=-\frac{C_2}{27};\quad \alpha_2=-\frac{40C_2}{27};\quad \alpha_3=\frac{5C_2}{27}\,. \tag{8}$$

Substituting Eq. (7) and Eq.(8) into Eq.(6), one can obtain the following expression for the stresses:

$$\sigma_1=\sigma_{11}=C_1\int_{-\infty}^{t} G(t-\tau)e^{Q_{VE}}F_1(\lambda)\frac{d\lambda}{d\tau}d\tau-p\,, \tag{9}$$

$$F_1(\lambda)=\left[\left(\frac{C_2}{27}\right)^2\left(-4\lambda^2+84-\frac{80}{\lambda}\right)\left(-4\lambda^3+84\lambda-40-\frac{30}{\lambda^2}-\frac{10}{\lambda^3}\right)+\left(\frac{8C_2}{27}\right)\left(-\lambda+\frac{10}{\lambda^2}\right)\right]; \tag{10}$$

$$Q_{VE}=\frac{C_2}{27}[-\lambda^4+42\lambda^2-40\lambda-36+\frac{30}{\lambda}+\frac{5}{\lambda^2}]; \tag{11}$$

$$\sigma_2=\sigma_3=\sigma_{22}=C_1\int_{-\infty}^{t} G(t-\tau)e^{Q_{VE}}F_2(\lambda)\frac{d\lambda}{d\tau}d\tau-p\,, \tag{12}$$

$$F_2(\lambda)=\left[10\left(\frac{C_2}{27}\right)^2\left(-4\lambda^2+3+\frac{1}{\lambda}\right)\left(-4\lambda^3+84\lambda-40-\frac{30}{\lambda^2}-\frac{10}{\lambda^3}\right)+\left(\frac{10C_2}{27}\right)\left(8\lambda+\frac{1}{\lambda^2}\right)\right]. \tag{13}$$

In the above derivations, the uninvolved off-diagonal relaxation functions are assumed to be zero; the diagonal relaxation functions are the same due to the assumption of isotropy, i.e. $\mathrm{G_{11}}=\mathrm{G_{22}}=\mathrm{G_{33}}=\mathrm{G}$. Since there is no other external stress except the tensile stress along the elongation direction, the stresses along the perpendicular directions, i.e. σ_2 and σ_3 in Eq. (12)

must be zero. The pressure p is thus determined and substituted back to Eq.(9) to obtain the tensile stress σ_1, i.e.,

$$\sigma_1 = \sigma_{11} = C_1 \int_{-\infty}^{t} G(t-\tau) e^{Q_{VE}} [F_1(\lambda) + F_2(\lambda)] \frac{d\lambda}{d\tau} d\tau \quad . \tag{14}$$

The final step is to determine the relaxation function $G(t-\tau)$. In this connection, a one-dimensional standard model was introduced by (Fung 1994) to derive a linear reduced relaxation function with a continuous spectrum, given by: $G(t) = \dfrac{1 + \int_0^\infty S(q) e^{-t/q} dq}{1 + \int_0^\infty S(q)\, dq}$. (15)

The relaxation spectrum S(q) denotes the amplitude of the viscous dissipation subject to the frequency 1/q. For many biological materials that exhibit viscoelastic behavior and low sensitivity to strain rates, the designation of the spectrum with constant amplitude over a range of frequency is found to fit the experimental results fairly well; the spectrum assumes the following form:

$$S(q) = \frac{C0}{q}, \quad \text{for } q_{1C} \le q \le q_{2C}$$
$$S(q) = 0, \quad \text{otherwise} \tag{16}$$

The parameters C0, q_{1C} and q_{2C} used in Eq. (16) can be determined experimentally by examining the stress relaxation of the tissues under constant strain or by experiments of dynamic loading. In this study, we adopt the parameters obtained from the study of subcutaneous tissues of rats under uniaxial tension (Iatridis et al 2003.). It was reported that C0=0.25, q_{1C}=1.86 second, and q_{2C}=110.4 second. Combining Eq. (9) – Eq.(16), one can solve numerically for the viscoelastic stress-time, stress-strain relations for various tissues undergoing the deformations according to the design of the experiment.

Corresponding Author: Chien-Yueh Huang, Email: mhuang@adm.njit.edu
Phone: 973-596-5613. Fax: 973-596-8436